

Ionization and temperature dependent attachment cross section measurements in C_3F_8 and C_2H_3Cl

P. J. Chantry and C. L. Chen^{a)}

Westinghouse R&D Center, 1310 Beulah Road, Pittsburgh, Pennsylvania 15235

(Received 18 October 1988; accepted 18 November 1988)

Total ionization and attachment cross sections have been measured in C_3F_8 at 330 K using an electron beam and a total ion collection technique, calibrated by similar measurements on N_2O and Xe. Our total ionization cross section is similar in general shape to a previous measurement of this type, but with typically half the magnitude. The ionization threshold cannot be accurately derived from these measurements, due to severe upward curvature immediately above threshold. The positive-ion signal rises above the background at 13.0 ± 0.1 eV, to be regarded as a lower limit to the true threshold. An overall ionization cross section with a threshold at 13.3 eV is recommended, based on threshold data from photoelectron spectroscopy and the present data between 14 and 80 eV. The room temperature total attachment cross section peaks at 2.8 eV with a value of 1.75×10^{-17} cm². This is 14 times smaller than the only other measurement of this type we are aware of. There is much better agreement with two more recently reported values unfolded from swarm experiments. The temperature dependence of the predominant dissociative attachment process, involving F^- production, was studied in a different apparatus using a mass filter and ion pulse counting. At 730 K the peak cross section has increased by $\sim 60\%$ and the threshold is lower by 1.1 eV. This second type of measurement was used to study the predominant dissociative attachment process in C_2H_3Cl , involving Cl^- production. At 290 K this has a threshold at 0.85 eV and a peak at 1.35 eV of 3.2×10^{-17} cm², in good agreement with recent work elsewhere. At 850 K the cross section at the peak is 2.6 larger, and lower in energy by 0.33 eV, while at 0 eV it has reached 6×10^{-18} cm². At higher temperatures effects ascribed to thermal dissociation of the C_2H_3Cl were observed. The implications of the present results regarding the use of these gases in diffuse discharge switches are discussed.

I. INTRODUCTION

The primary objective of the work reported here was to measure the attachment cross sections for the subject gases and establish their sensitivity to gas temperature. Our interest in these gases stems from their possible use as optically controlled attaching additives in an externally sustained diffuse gas discharge switch.¹ In this application the switch medium is required to cause minimal electron loss rate when the switch is in the conducting phase, but to recover its insulating properties as rapidly as possible when the external source of ionization is turned off. During the recovery the electron density in the medium must decrease while the switch voltage, and consequently the electric field experienced by the electrons, are increasing. As the gas pressures employed the electrons remain essentially in equilibrium with the field during the switch recovery, and as a consequence, their mean energy increases from typically a few tenths of an eV to a few eV. It is therefore desirable that the medium's net attachment rate be small for low electron energies, and increase rapidly with mean energy above a few tenths of an eV. With these and other considerations in mind, possible candidates can be identified² for consideration and further testing³ as attaching additives.

Additional improvement in switch performance can in principle be realized by optically enhancing the attachment rate in the medium during the recovery phase. Possible means of achieving this are (i) by photodissociation causing formation of strongly attaching neutral fragments,⁴ (ii) by short-wavelength optical excitation of higher energy electronic states,⁵ or (iii) by vibrational excitation of the attachers by tuned infrared irradiation.^{6,7} In the present work we investigate two possible candidates for the third of these approaches. They were chosen on the basis of the existing knowledge regarding their attaching properties, such that they would be expected to have the type of passive attachment behavior described above, and from their infrared absorption spectra,⁸ which are such that one may plan to use a CO_2 laser as an efficient source for the excitation. As a first step in screening these and other candidates, it is important to establish the sensitivity of their attachment cross sections to nonselective vibrational excitation, achieved by simply heating the gas. In addition, it is important to establish the shape and magnitude of the attachment cross section for the "cold" gas in order that the electron transport properties of the switch medium may be properly modeled by a Boltzmann or Monte Carlo code analysis.

There is considerable prior literature on the attachment properties of C_3F_8 , including a total attachment cross-section measurement⁹ made by the classical Tate and Smith¹⁰ technique. When starting the present study we anticipated confirming the validity of that measurement, and moving

^{a)} Present address: Brookhaven National Laboratory.

quickly to the study of the temperature sensitivity of the process. However, our initial cross-section measurements revealed a surprisingly large discrepancy, exceeding an order of magnitude, in the peak magnitude. Because of this we determined that a more extensive series of room temperature measurements was needed to provide more definitive cross-section data, for both total attachment and total ionization. The results of that study, and subsequent measurements conducted at elevated gas temperatures, are reported here. Since the initiation of this study, swarm experiments conducted elsewhere^{11,12} have yielded C_3F_8 attachment cross-section data with which the present results may be compared.

The information available on C_2H_3Cl included a number of recent electron beam studies of both negative ion production¹³⁻¹⁶ and electron scattering.^{16,17} In the present context the paper of Stricklett *et al.*¹⁶ is particularly interesting in that it implicitly contains a measurement of the peak attachment cross section, relative to the known value for O^- production from CO_2 . Also, these authors argue, and proceed to demonstrate, that the process of dissociative attachment in the chloroethylenes should be enhanced by out-of-plane positioning of the Cl atom. By analogy, Burrow¹⁸ has suggested that excitation of internal vibrational modes causing such a distortion in C_2H_3Cl could lead to significant enhancement of its attachment cross section. Based on this information and the known IR absorption properties, this molecule was clearly of sufficient interest to be included in the study.

In Sec. II we describe the experimental techniques used for the present measurements, the results being presented in Sec. III. The relation of these results to other available data, and the implications regarding the possibilities of employing these gases as attaching additives, are discussed in Sec. IV. The results and conclusions drawn from this study are summarized in Sec. V.

II. EXPERIMENT

In the present study measurements were performed with two types of apparatus. The first apparatus permits measurements of the total ion current as a function of the absolute pressure in the collision chamber. Comparison of these signals with others, obtained similarly using a gas for which the cross section is known, provides a measure of the absolute cross section. The second type of measurement employs a "high-temperature tube" having a heatable collision chamber which allows us to measure the dependence of the ion production processes on the gas temperature. In both cases the electron beam is produced by a directly heated filament and an electron gun employing the retarding potential difference (RPD) technique^{19,20} to enhance the energy resolution. With either apparatus mass-analyzed ion detection can be performed using a quadrupole mass filter employing ion-counting techniques. In the measurements reported here this feature was used exclusively with the high-temperature tube. These techniques are described here only briefly, details being given only of those aspects which have not been described in previous publications.

A. Total ion collection cross section measurements

We have used this approach in the past to measure attachment cross sections in various gases including CO ,²¹ SF_6 ,²² F_2 , and NF_3 ,²³ and some of the details of the technique may be found in these references. The collision chamber and ion collection electrode geometry used for these measurements is shown to scale in Fig. 1, which represents a section perpendicular to the electron beam through the center of the collision chamber. The chamber is machined from a stainless steel block and is gold plated. All associated electrodes are supported directly from the block, including those constituting the electron gun and electron beam collector electrodes which are not shown in this view. The electron beam enters and leaves the chamber through ample apertures whose potentials are nominally identical to the chamber potential. Ions formed within the chamber by the electron beam experience a transverse extraction field applied by the parallel plate repeller and attractor electrodes. The dependence of the collected ion signal on the magnitude of this field is recorded for each process studied. Subsequent quantitative measurements of the ion current are made with the extrac-

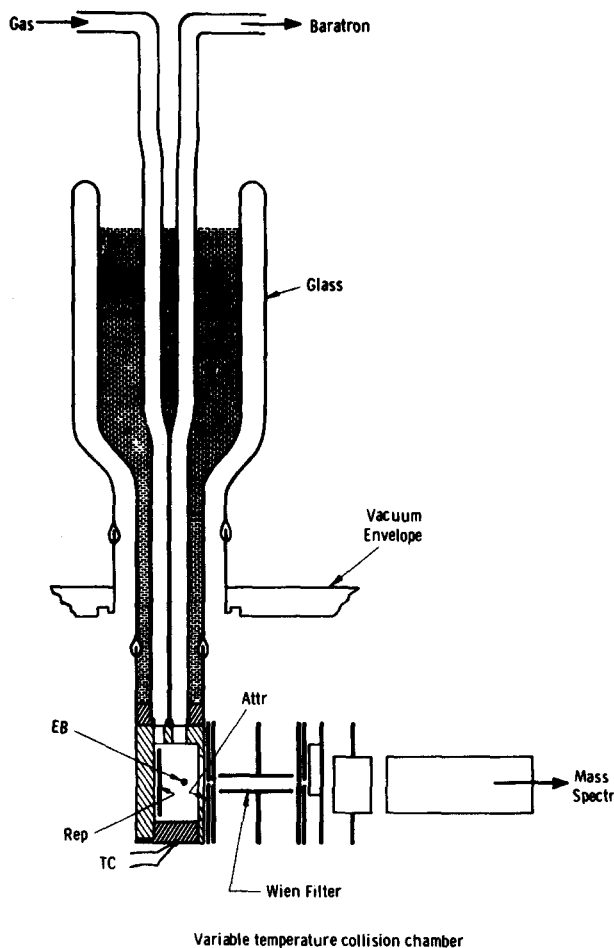


FIG. 1. Collision chamber and related electrodes used for the room temperature measurements of the cross-section magnitudes. The electron beam (EB) is produced by an electron gun (not shown). The repeller (Rep) and attractor (Attr) electrodes form a parallel plate geometry for the total ion current measurements.

tion field set at a value adequate for the signal to be only weakly dependent on the field. Care is also taken to adjust the repeller and attractor potentials relative to the chamber potential such that the electron beam has its minimum energy within the chamber. This ensures that we are able to operate the beam down to essentially zero electron energy, and that the electron-retarding curve will provide a reliable zero energy scale calibration point. An externally controlled magnetic field of a few hundred gauss is imposed parallel to the electron beam. This serves to align the beam and constrain it to an essentially equipotential surface within the chamber. The magnetic field also serves the Wien velocity filter, but the latter was not used significantly in the present study.

Two holes in the top of the collision chamber match similar holes in the stainless steel base of a Dewar vessel to which it is connected in good thermal contact. There are two metal tube connections to the collision chamber. One allows gas to be fed to the chamber, while the other allows the chamber pressure to be measured using a Baratron capacitance manometer. The gas and collision chamber temperature can be controlled by use of appropriate fluids in the Dewar vessel.

B. Mass resolved and elevated temperature measurements

We have used this "high-temperature tube" in the past to measure both positive and negative fragment ion cross sections in various gases including N_2O^{24} and SF_6^{22} and to study the temperature dependence of such reactions. Details of the technique may be found in Chantry,²⁴ and reference may be made particularly to Fig. 3 therein. In this case the collision chamber consists of an iridium tube of length 5 cm.

Gas admitted to the collision chamber escapes through two apertures used to pass the electron beam through the collision chamber, and a third slit in the sidewall which allows a sample of the ions to escape perpendicularly to the electron beam.

The electron beam is aligned by an externally applied magnetic field of about 500 G. The collision chamber is rigidly mounted to a glass plate and can be heated by passing a high (0–100 Å) direct current through the collision chamber. A platinum, platinum/rhodium thermocouple is spot welded to the outer surface of the collision chamber wall opposite the ion exit slit and is used to monitor the chamber temperature.

The electron gun and electron beam collection optics assemblies are mounted on a *U* bracket which is placed around the collision chamber. The *U* bracket independently maintains the alignment of the gun and collection optics, and provides a convenient means to align the electron gun system to the collision chamber.

The collision chamber is surrounded by a similar tube of larger dimension which acts as a radiation shield (RS). The radiation shield can be biased relative to the collision chamber to permit extraction of the proper polarity ions through an aperture in the side of the collision chamber. Two planar grids outside of the ion extraction aperture are situated so that an electric field, perpendicular to the magnetic field, can be produced to prevent deflection of the extracted ions by the fringing magnetic field used to align the electron beam. The extracted ion sample is subsequently focused through a differential pumping aperture into a chamber housing the quadrupole mass filter. The mass-selected ions impinge on a channeltron multiplier used in a pulse-counting mode. Care is taken to saturate the ion count

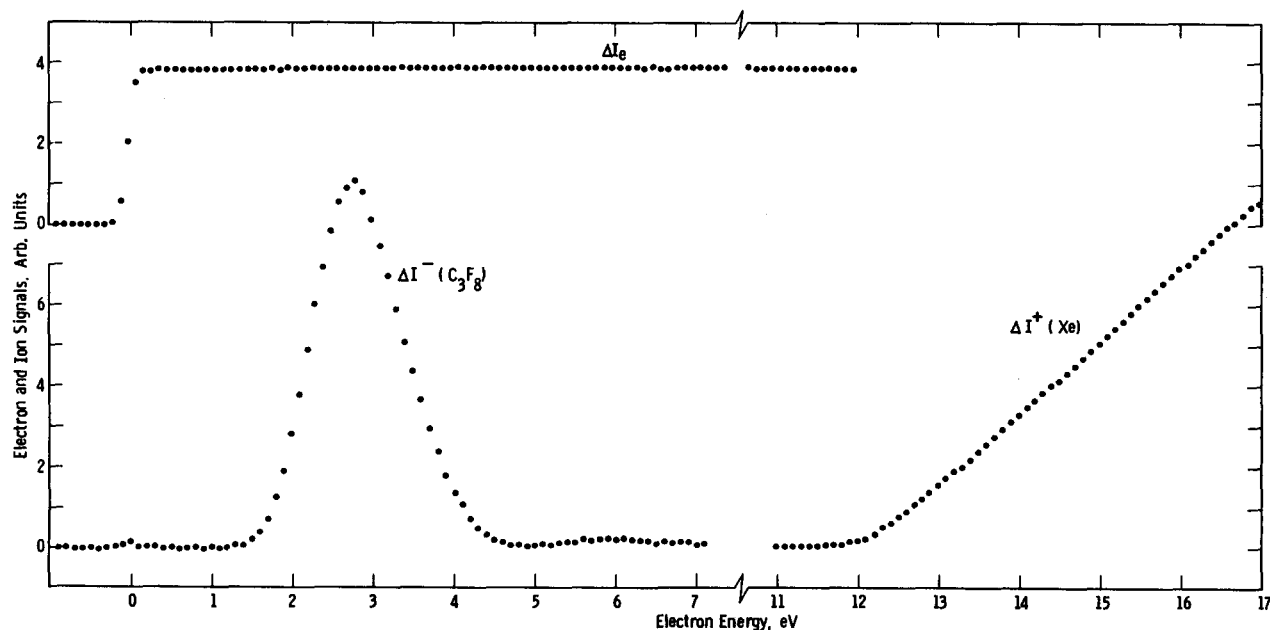


FIG. 2. Composite figure showing the electron energy dependence of the negative-ion signal from C_3F_8 , the positive-ion signal from Xe, and the RPD electron beam current. The relative positions of the three curves are given directly by the measurements. The position of the scale zero is adjusted to coincide with the steepest part of the retarding curve.

rate by operating the channeltron at sufficient voltage, and the mass filter such that the ion signal strength is not significantly dependent on the mass resolution. With these measures the mass discrimination of the system is minimized.

III. RESULTS

A. Perfluoropropane, C_3F_8 , measurements

An example of data obtained with C_3F_8 in the total collection tube is shown in Fig. 2. The three curves indicate "difference" signals of the transmitted electron beam, the negative-ion signal collected at the positively biased electrode, and the positive-ion signal collected at the opposing electrode, all measured under identical operating conditions of the tube. The energy scale, obtained in this case by setting zero at the steepest part of the electron beam-retarding curve, gives the expected threshold for Xe^+ production, 12.13 eV, to within the target accuracy of ± 0.1 eV.

In order to place the total ion current measurements on a cross-section scale, calibration measurements of the type illustrated in Fig. 3 were performed. The peak attachment cross section in C_3F_8 is here calibrated against the known peak cross section for O^- production from N_2O . The two signals are measured under the same collision chamber conditions, with the extraction electrode potentials chosen as described above. The ratio of the slopes (2.03) is multiplied by $8.6 \times 10^{-18} \text{ cm}^2$, the known cross section for O^- produc-

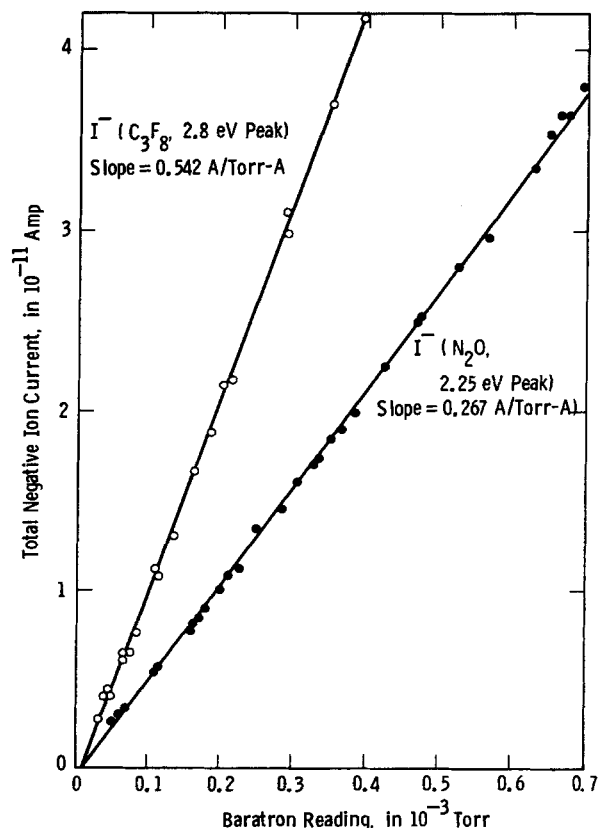


FIG. 3. An example of the total negative ion currents measured as a function of the collision chamber pressure in N_2O and C_3F_8 . In each case the electron beam energy is adjusted to the peak in the cross section. The ratio of the slopes gives the ratio of the peak cross sections.

tion from N_2O ,²⁵ to give the value of the peak attachment cross section of C_3F_8 , $1.75 \times 10^{-17} \text{ cm}^2$.

Similar calibration measurements were performed for the positive ion signals, using Xe as the calibrant gas, together with the cross-section measurements of Rapp and Englander-Golden.²⁶ In Fig. 4(a) the full curve shows the cross-section shape, measured by scanning the electron energy at a fixed pressure, and normalized to the points at 40, 60, and 80 eV obtained from pressure scans of the type shown in Fig. 3. Figure 4(b) shows a more-detailed view of the data recorded

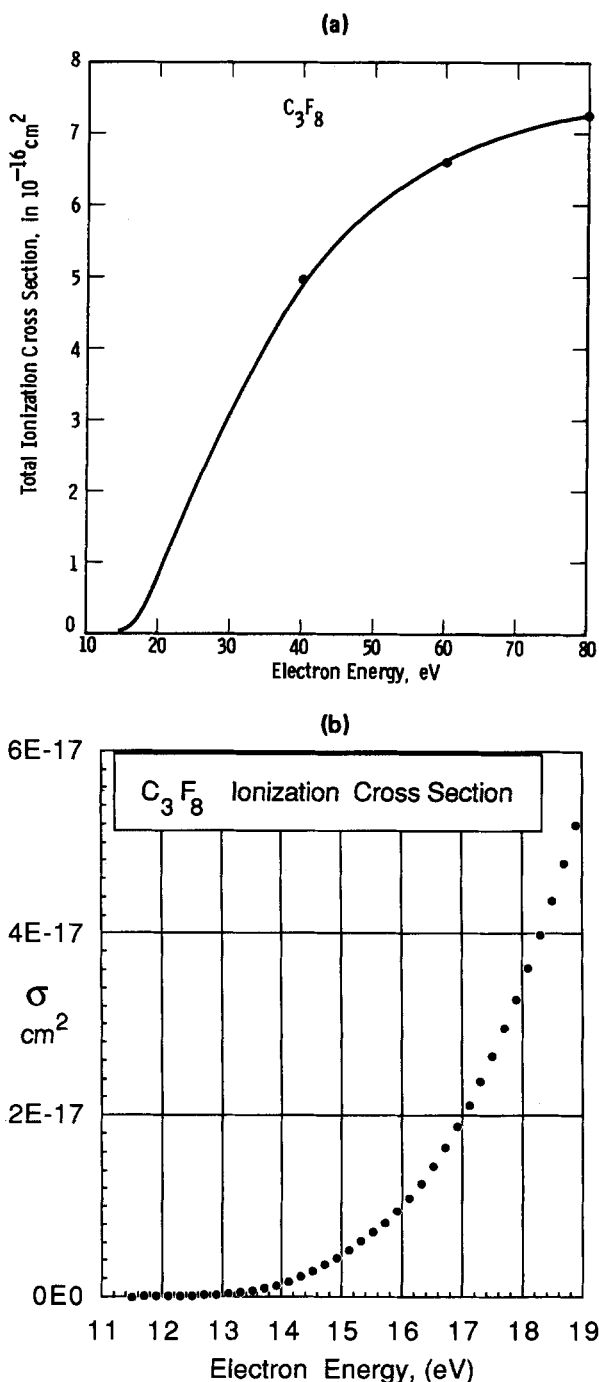


FIG. 4. The total ionization cross section of C_3F_8 measured relative to the known cross section of Xe. In (a) the full curve shows the shape of the cross section measured at a fixed pressure, normalized to the points at 40, 60, and 80 eV determined by measurements over a range of pressure of the type shown in Fig. 2. In (b) we show details of the threshold region.

in the region immediately above threshold. The severe curvature makes a determination of the true threshold somewhat difficult. We obtain from our measurements a value of 13.0 ± 0.1 eV.

Our total negative ion measurements at $T = 330$ K give the calibrated attachment cross-section data for C_3F_8 shown on a linear plot in Fig. 5. This same result is plotted semilogarithmically as the full curve in Fig. 6, together with two recently published results.^{11,12}

Additional mass-resolved data were taken using the high-temperature tube. With no direct heating the collision chamber has a normal operating temperature close to 290 K, with the electron gun operating. This is slightly below room temperature due to its location above a large liquid nitrogen-cooled trap. Under these "room-temperature" conditions, measurements were made of the F^- appearance curve and of the O^- appearance curve using mixtures of C_3F_8 and N_2O in the collision chamber. The separation of these peaks confirmed the position of the F^- peak at 2.8 eV.

The data on F^- from C_3F_8 obtained at room temperature and at various elevated temperatures using the high-temperature tube are shown in Fig. 7 as the family of full curves. These curves were placed on an absolute magnitude scale by setting the room temperature peak value equal to the value of 1.75×10^{-17} cm² determined above. The relative magnitudes of the curves taken at different temperatures were determined by also measuring at each temperature the strength of the CF_3^+ signal produced by 97 eV electrons, and assuming that production of this ion from C_3F_8 is temperature insensitive at this energy.

B. Vinyl chloride, C_2H_3Cl , measurements

Measurements on vinyl chloride were performed only in the high-temperature tube. As reported previously by oth-

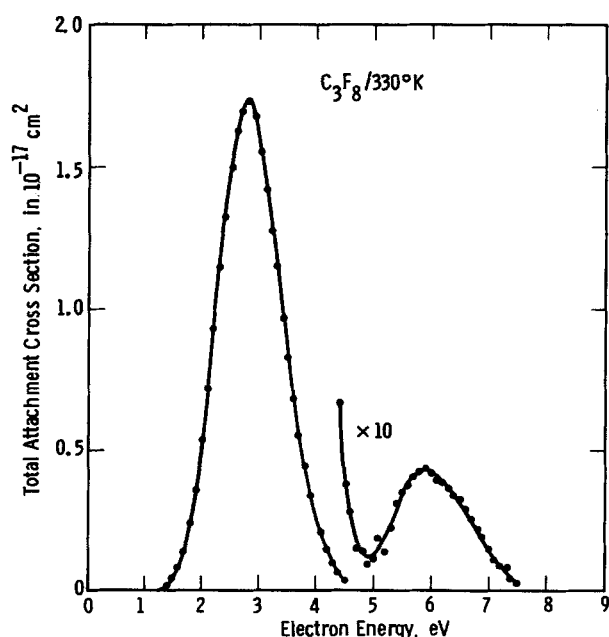


FIG. 5. The total attachment cross section of C_3F_8 measured at 330 K relative to the known cross section of N_2O .

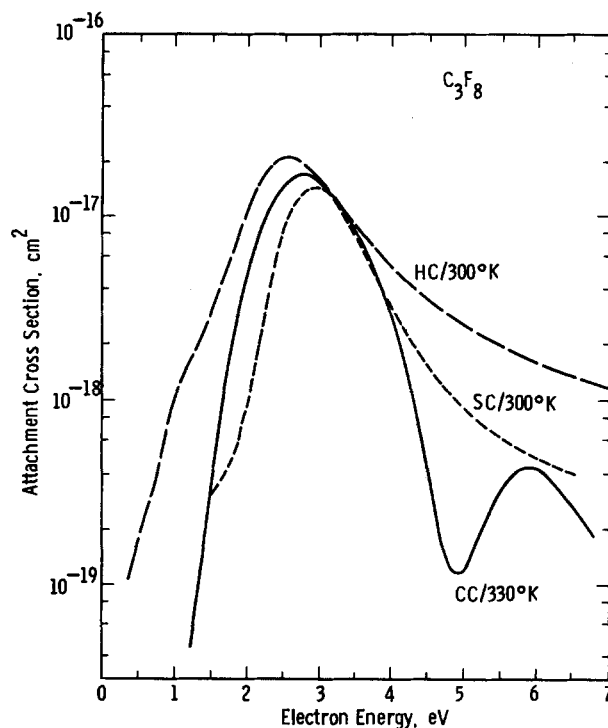


FIG. 6. Comparison of the present measurement of the room temperature attachment cross section in C_3F_8 with data of Spyrou and Christophorou (SC, Ref. 12), and of Hunter and Christophorou (HC, Ref. 11).

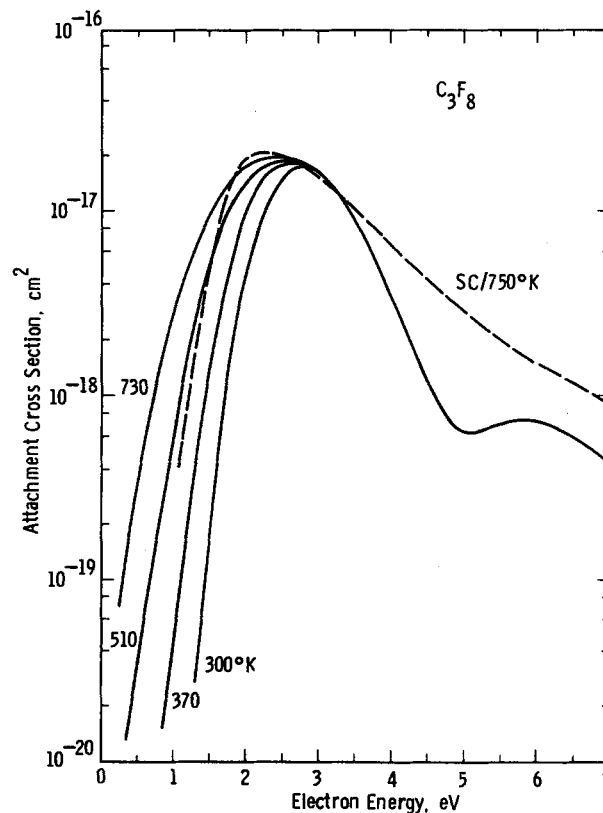


FIG. 7. The cross section for F^- production from C_3F_8 measured at the temperatures indicated, using the "high-temperature collision chamber." The data of Spyrou and Christophorou (SC, Ref. 12) is shown for comparison.

ers,^{13,14} the only ion formed in significant amounts is Cl^- . The strength of the mass-resolved peak Cl^- signal was measured under room-temperature conditions as a function of the gas pressure in the line supplying the collision chamber. Comparison of these measurements with similar measurements of the O^- signal produced from N_2O gave a value of $3.2 \times 10^{-17} \text{ cm}^2$. The position of the peak at 1.35 eV was determined relative to the steepest point of the electron-retrarding curve. This energy calibration procedure could not be routinely relied on but was found to be satisfactory provided the collision chamber was cleaned by prior heating. The resulting cross-section curve is shown as a linear plot in Fig. 8. The peak has a FWHM of 0.60 eV.

The results of measurements performed at room temperature and at various elevated temperatures are summarized in the semilog plot in Fig. 9. These curves were placed on a magnitude scale by setting the 290 K peak equal to the value of $3.2 \times 10^{-17} \text{ cm}^2$ determined above. The relative magnitudes of the curves taken at different temperatures were determined by also measuring at each temperature the strength of the parent positive-ion signal, produced by 38 eV electrons, and assuming that this ion production process is temperature insensitive. At temperatures above 850 K we found the reference $C_2H_3Cl^+$ signal decreased significantly, and tentatively ascribed this to thermal dissociation of the vinyl chloride. An instrumental effect, such as a temperature dependent bypass leak from the collision chamber, was ruled out by repeating the measurements with a fixed ratio mixture of C_2H_3Cl and Ne flowing through the collision chamber, and monitoring both the $C_2H_3Cl^+$ and the Ne^+ signals as the temperature was raised. The anomalous drop in the $C_2H_3Cl^+$ signal was not present in the Ne^+ signal. Thus, we conclude that the highest temperature data, shown in Fig. 9 as a broken curve, is taken in the presence of thermal dissociation of the C_2H_3Cl . The direction of the additional uncertainty attached to this curve is not obvious, since we have no independent knowledge of the Cl^- production pro-

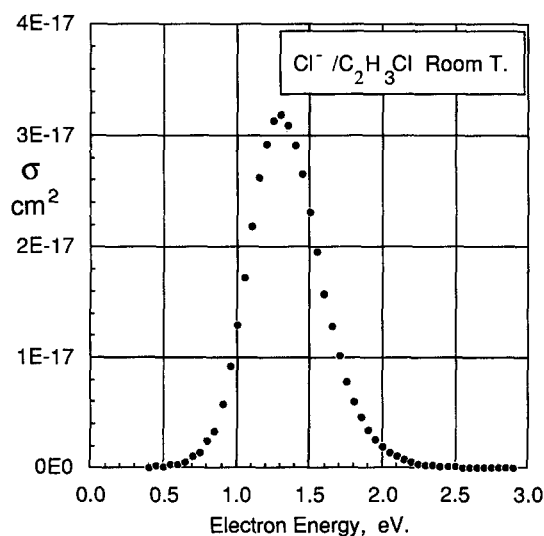


FIG. 8. The cross section for Cl^- production from C_2H_3Cl at room temperature (330 K).

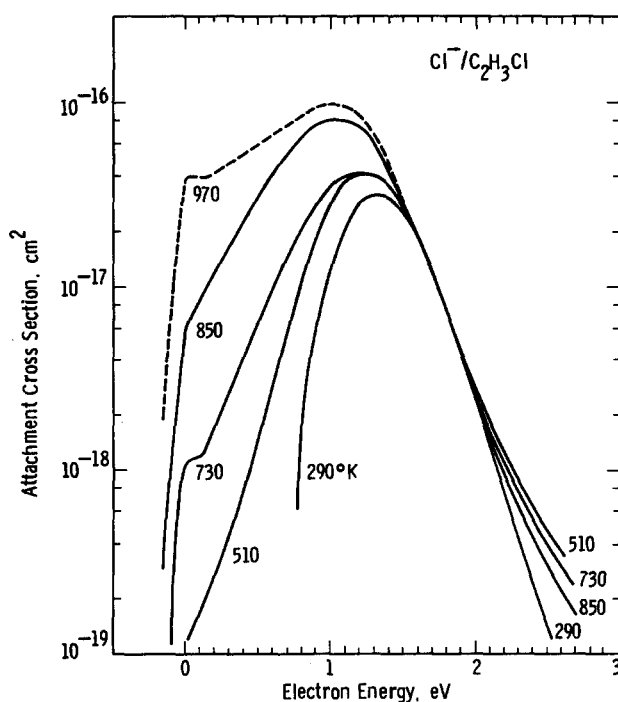


FIG. 9. The cross section for Cl^- production from C_2H_3Cl measured at the temperatures indicated, using the high-temperature collision chamber. The highest temperature curve (970 K) is uncertain due to thermal dissociation effects.

cesses from the thermal dissociation products. In the event that the products do not produce Cl^- at these energies, the broken curve would represent a lower limit to the C_2H_3Cl cross section at this temperature.

IV. DISCUSSION

The determination of ion appearance potentials from ion appearance curves is in essence a deconvolution problem. Normally it is possible to adopt the simple approach of linearly extrapolating the curve measured immediately above threshold. For confidence to be placed in the extrapolated threshold determined in this way it is necessary that the range of the linear fit be at least a few times the energy resolution of the measurement, and that the residual curvature at the "toe" of the curve be consistent with the known energy resolution of the measurements.²⁷ The appearance curve for positive ions from C_3F_8 measured in the present work does not meet these criteria, due to the severe upward curvature, and consequently it is difficult to place reasonable confidence limits on the determined value of 13.0 eV. This number corresponds to the most probable electron beam energy at which the signal rose significantly above the background. Given the sensitivity of these measurements, and the possible presence of "hotbands," it is reasonable to regard this value as a lower limit to the true value with the possible error being at least as large as the energy resolution, in this case 0.1 eV.

The difficulty of making this determination is inherent in the process and is no doubt partly responsible for the wide range of previously measured values. Lifschitz and Gra-

jower²⁸ used a mass spectrometer to measure a threshold of 13.4 eV for the production of CF_3^+ . These authors list prior values ranging to 14.65 eV, not including Kurepa's value of 14.7 eV, and calculate a value of 13.3 eV to be expected from known heats of formation. The value of 13.38 eV obtained by photoelectron spectroscopy²⁹ appears to be the most reliable. For the purposes of computing ionization rates in a discharge environment, we would therefore recommend use of our determined cross section down to an electron energy of approximately 14 eV, and matching this curve to one going to zero at 13.3 eV. This procedure gives the values listed in Table I.

The present room temperature cross sections for C_3F_8 determined by total ion current measurements may be compared with the results of Kurepa,⁹ who used the same general technique. His positive ionization cross-section data are not reported in sufficient detail to compare them with the present results in the threshold region. There is reasonably good agreement regarding the general shape up to 80 eV, which was the limit of the present measurements. However, Kurepa's cross section is approximately a factor of 2 larger than the present measurement. Discrepancies of this magnitude between measurements of this type are not normally encountered, and we can offer no explanation in this case.

Comparison with Kurepa's total attachment cross section is best made by plotting the data semilogarithmically, as in Fig. 6. To this end, Fig. 4 of Ref. 9 was replotted and overlaid on the present Fig. 6. The shapes of the two measured cross sections are found to be in excellent agreement over most of the main peak, but compared to the main peak we find the amplitude of the second peak to be smaller by a factor of 39, while Kurepa's data indicate a factor of 22. More serious is the disagreement regarding the position and magnitude of the main attachment peak. Kurepa's data show this to have a magnitude of $2.3 \times 10^{-16} \text{ cm}^2$ occurring at 3.3 eV, compared with the present values of $1.75 \times 10^{-17} \text{ cm}^2$ and 2.8 eV. We are unable to explain these discrepancies.

TABLE I. Total ionization cross section of perfluoropropane.

Electron energy (eV)	Cross section (cm ²)	Electron energy (eV)	Cross section (cm ²)	Electron energy (eV)	Cross section (cm ²)
13.3	0.00E 0	16.5	1.45E - 17	24	1.74E - 16
13.5	4.44E - 19	16.7	1.66E - 17	26	2.20E - 16
13.7	8.89E - 19	16.9	1.88E - 17	28	2.66E - 16
13.9	1.33E - 18	17.1	2.12E - 17	30	3.08E - 16
14.1	1.77E - 18	17.3	2.38E - 17	32	3.49E - 16
14.3	2.32E - 18	17.5	2.66E - 17	34	3.87E - 16
14.5	2.93E - 18	17.7	2.96E - 17	36	4.25E - 16
14.7	3.64E - 18	17.9	3.29E - 17	40	4.88E - 16
14.9	4.42E - 18	18.1	3.63E - 17	45	5.51E - 16
15.1	5.29E - 18	18.3	3.99E - 17	50	5.97E - 16
15.3	6.20E - 18	18.5	4.38E - 17	55	6.35E - 16
15.5	7.20E - 18	18.7	4.78E - 17	60	6.60E - 16
15.7	8.34E - 18	18.9	5.20E - 17	65	6.84E - 16
15.9	9.64E - 18	19	5.40E - 17	70	7.02E - 16
16.1	1.11E - 17	20	7.80E - 17	75	7.17E - 16
16.3	1.27E - 17	22	1.25E - 16	80	7.30E - 16

In Fig. 6 the present data may be compared directly with the "swarm-unfolded" attachment cross sections derived from measurements^{12,11} of the attachment coefficient in dilute mixtures of C_3F_8 in N_2 or Ar. At the pressures used in both these studies there is a contribution to the measured attachment from the initial transient parent negative-ion species. This contribution is included in the data of Hunter and Christophorou,¹¹ and for this reason their curve is expected to lie above the present data at the lower energies. At higher energies parent ion production is much less likely, and the differences seen above 4 eV may indicate a real discrepancy. Better overall agreement is found with the data of Spyrou and Christophorou.¹² In this case the basic data also included a contribution to the measured attachment rate from the transient parent ion, and they similarly derived an unfolded cross section which included this contribution. In addition, on the basis of their temperature dependence measurements, these authors assigned relative contributions to the two processes and derived cross sections for the dissociative contribution at each of the temperatures studied. It is this cross section which is reproduced in Fig. 6. The agreement between these data and the present result is already fairly good, and would clearly be improved for energies below 3 eV if a larger fraction of the measured total attachment coefficient was assigned to the dissociative process.

In Fig. 7 the cross section obtained in the present work at 730 K may be compared with the data from Ref. 12 taken at 750 K, where we have again plotted their derived cross section for the dissociative contribution to the measured attachment rate. The agreement in the peak magnitude is very good, considering the difficulties involved in both determinations, and as in the room temperature data the agreement could clearly be improved below 2 eV if a larger fraction of the measured total attachment rate was assigned to the dissociative process. It should perhaps be emphasized that the present type of measurement normally will measure the shape of the cross section with very high confidence levels, as evidenced by comparing results from various laboratories.

The room temperature measurements of Cl^- production from C_2H_3Cl may be compared directly with recent high-resolution electron beam measurements from a number of sources.¹³⁻¹⁶ These papers also provide comparisons of the dissociative attachment processes in a number of chemically related compounds and discuss the implications regarding the molecular states involved. Including the present work, all these measurements find the same peak energy for Cl^- production from C_2H_3Cl within the combined error bars, and all but one¹⁵ place it between 1.31 and 1.37 eV. Similar agreement exists regarding the peak FWHM (0.60 eV).

The present measurement of the peak cross-section magnitude, $3.2 \times 10^{-17} \text{ cm}^2$, is in excellent agreement with the value of $3.5 \times 10^{-17} \text{ cm}^2$ implicit in the results of Stricklett *et al.*¹⁶ We note that these authors performed a total ion collection measurement, in contrast with the present measurement performed with a mass filter. In general the latter type of measurement has significantly greater uncertainties due to the possible presence of mass or ion translational energy discrimination effects. In this case we note that Dressler *et al.* have shown that the Cl^- fragment is formed with little

translational energy, typically 0.1 eV, independent of the electron energy used. Olthoff *et al.* report a similar result. In these circumstances the discrimination effects associated with a mass filter are greatly reduced, and with care can be eliminated. Greater reliance can then be placed on cross-section measurements performed in this way.

It is clear from Figs. 7 and 9 that in both these gases the dissociative attachment process is significantly dependent on gas temperature, and thus both these gases are of interest regarding possible photoenhancement of this process by IR absorption. Of the two, C_2H_3Cl has the stronger dependence on temperature and for this reason might be considered the better candidate. However, it must be kept in mind that in the application of present interest, discussed in the Introduction, the attaching species must be reasonably stable in the discharge. In the present work C_3F_8 demonstrated greater stability against thermal dissociation, and similar differences might well be found in the discharge environment. Thus, the present results do not significantly favor one candidate over the other in choosing an attaching discharge additive. The results of experiments to determine the possibility of enhancing their attachment by irradiation at CO_2 laser wavelengths, as was achieved previously in SF_6 , will be reported elsewhere.

V. SUMMARY AND CONCLUSIONS

The measurements reported above provide ionization and attachment cross sections for C_3F_8 which are much smaller than previously reported measurements⁹ which used essentially the same technique. Based on the present measurements of the general shape and magnitude of the ionization cross section, and a more reliable threshold value determined by photoelectron spectroscopy,²⁹ we recommend an ionization cross section up to 80 eV which incorporates the best information available at this time.

There is relatively good agreement between the present measurements of the C_3F_8 attachment cross section at room temperature and at elevated temperatures, and the results obtained from swarm experiments.^{11,12} The present results suggest that, in the interpretation of the swarm measurements, a smaller fraction of the overall attachment rate should be assigned to the parent ion process at the lower electron energies. The C_3F_8 attachment cross section is significantly dependent on gas temperature, but not dramatically so in the way that has been observed with some molecules.²⁴ There were no effects of thermal dissociation of the C_3F_8 apparent in the present study.

The present room temperature measurement of the cross section for Cl^- production from C_2H_3Cl gives a peak at 1.35 eV with a FWHM of 0.6 eV, and a peak value of $3.2 \times 10^{-17} \text{ cm}^2$. These numbers agree well with a number of recent determinations of the shape and position in energy of the peak, and also with a total attachment cross-section measurement¹⁶ which gave a value of $3.5 \times 10^{-17} \text{ cm}^2$.

The effects of increased temperature on the attachment cross section are significantly greater in the case of C_2H_3Cl than with C_3F_8 . At 850 K the peak cross section has increased by a factor of 2.6 and occurs lower in energy by 0.3 eV. The threshold has moved from 0.85 eV to zero energy,

where its value becomes $6 \times 10^{-18} \text{ cm}^2$. At higher temperatures the interpretation of the data becomes uncertain due to the presence of effects ascribed to thermal dissociation of the C_2H_3Cl .

The presently measured temperature sensitivities of the attachment processes in both these gases, and their known IR absorption spectra, make them interesting candidates for use as attaching additives in optically controlled discharges, but does not clearly identify the better choice. The effect of temperature is significantly greater for C_2H_3Cl , but the effects of thermal dissociation observed in the present work indicate the possibility of similar chemical stability problems in the gas discharge environment.

ACKNOWLEDGMENTS

We wish to acknowledge the technical assistance of W. M. Uhlig and L. D. Kurtz in the construction and maintenance of the apparatus, and thank the authors of Refs. 7 and 16 for communicating their results to us prior to their publication. This work was supported in part by the U. S. Army Research Office.

¹K. H. Schoenbach, G. Schaeffer, M. Kristiansen, L. L. Hatfield, and A. H. Guenther, IEEE Trans. Plasma Sci. **10**, 246 (1982).

²L. G. Christophorou, S. R. Hunter, J. G. Carter, and R. A. Mathis, Appl. Phys. Lett. **41**, 147 (1982).

³P. Bletzinger, Proc. 4th. Pulse Power Conf. Albuquerque, 1983, p. 37.

⁴M. J. Rossi, H. Helm, and D. C. Lorents, Appl. Phys. Lett. **47**, 576 (1985). O. Kobayashi, T. Sasagawa, and M. Obara, *ibid.* **51**, 2103 (1987).

⁵L. G. Christophorou, S. R. Hunter, L. A. Pinnaduwa, J. G. Carter, A. A. Christodoulides, and S. M. Spyrou, Phys. Rev. Lett. **58**, 1316 (1987).

⁶C. L. Chen and P. J. Chantry, J. Chem. Phys. **71**, 3897 (1979).

⁷G. Schaefer, M. Giesselmann, B. Pashaie, and M. Kristiansen, J. Appl. Phys. **64**, 6123 (1988).

⁸Matheson Gas Data Book.

⁹M. V. Kurepa, 3rd Czech Conference on Electronics and Vacuum Physics Transactions, 1965, p. 107.

¹⁰J. T. Tate and P. T. Smith, Phys. Rev. **39**, 270 (1980); see also Ref. 26.

¹¹S. R. Hunter and L. G. Christophorou, J. Chem. Phys. **80**, 6150 (1984).

¹²S. M. Spyrou and L. G. Christophorou, J. Chem. Phys. **83**, 2829 (1985).

¹³J. K. Olthoff, J. A. Tossell, and J. H. Moore, J. Chem. Phys. **83**, 5627 (1985).

¹⁴R. Dressler, M. Allan, and E. Haselbach, Chimia **39**, 385 (1985).

¹⁵R. Kaufel, E. Illenberger, and H. Baumgarter, Chem. Phys. Lett. **106**, 342 (1984).

¹⁶K. L. Stricklett, S. C. Chu, and P. D. Burrow, Chem. Phys. Lett. **131**, 279 (1986).

¹⁷P. D. Burrow, A. Modelli, N. S. Chiu, and K. D. Jordan, Chem. Phys. Lett. **82**, 270 (1981).

¹⁸P. D. Burrow (private communication).

¹⁹R. E. Fox, W. M. Hickam, D. J. Grove, and T. Kjeldaas, Rev. Sci. Instrum. **26**, 1101 (1955).

²⁰P. J. Chantry, Rev. Sci. Instrum. **40**, 884 (1969).

²¹P. J. Chantry, J. Chem. Phys. **57**, 3180 (1972).

²²L. E. Kline, D. K. Davies, C. L. Chen, and P. J. Chantry, J. Appl. Phys. **50**, 6789 (1979).

²³P. J. Chantry, in *Applied Atomic Collision Physics*, Vol. 3, *Gas Lasers*, edited by R. W. McDaniel and W. L. Nighan (Academic, New York, 1982).

²⁴P. J. Chantry, J. Chem. Phys. **51**, 3369 (1969).

²⁵D. Rapp and D. D. Briglia, J. Chem. Phys. **43**, 1480 (1965).

²⁶D. Rapp and P. Englander-Golden, J. Chem. Phys. **43**, 1464 (1965).

²⁷P. J. Chantry, J. Chem. Phys. **55**, 2746 (1971); **65**, 4412 (1976); Rev. Sci. Instrum. (to be published).

²⁸C. Lifshitz and R. Grajower, Int. J. Mass Spectrom. Ion Phys. **3**, 211 (1969).

²⁹M. J. S. Dewar and S. D. Worley, J. Chem. Phys. **50**, 654 (1969).